

Synthesis and DFT Studies of Pyrimidin-1(2*H*)-ylaminofumarate Derivatives

¹Murat Saracoglu*, ²Zulbiye Kokbudak, ¹M. Izzettin Yilmazer and ³Fatma Kandemirli

¹*Faculty of Education, Erciyes University, Kayseri, Turkey.*

²*Faculty of Science, Erciyes University, Kayseri, Turkey.*

³*Faculty of Engineering and Architecture, Kastamonu University, Kastamonu, Turkey.*

muratsaracoglu@gmail.com*

(Received on 17th July 2019, accepted in revised form 20th May 2020)

Summary: Pyrimidine derivatives have biological and pharmacological properties. Therefore, in this study we focused on the synthesis various Pyrimidine derivatives to make noteworthy contributions this class of heterocyclic compounds. In the present study, the new compounds (**4-6**) were obtained by the reactions of 1-amino-5-benzoyl-4-phenylpyrimidin-2(1*H*)-one (**1**), 1-amino-5-(4-methylbenzoyl)-4-(4-methylphenyl)pyrimidin-2(1*H*)-one (**2**) and 1-amino-5-(4-methoxybenzoyl)-4-(4-methoxyphenyl)pyrimidin-2(1*H*)-one (**3**) with dimethyl acetylenedicarboxylate. The structures of these compounds were proved by elemental analysis, FT-IR, ¹H and ¹³C-NMR spectra. In addition to, quantum chemical calculations were made to find molecular properties of the pyrimidin-1(2*H*)-ylaminofumarate derivatives (**4-6**) by using DFT/B3LYP method with 6-311++G(2d,2p) basis set. Quantum chemical features such as E_{HOMO}, E_{LUMO}, energy gap, ionization potential, chemical hardness, chemical softness, electronegativity etc. values for gas and solvent phase of neutral molecules were calculated and discussed.

Keywords: Pyrimidine Derivatives; Dimethyl Acetylenedicarboxylate; Synthesis; DFT; Quantum Chemical Calculations.

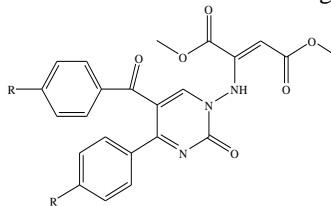
Introduction

Pyrimidines and their derivatives as important sensitive chemicals [1, 2] have been frequently found in many natural products and medicines, and have demonstrated a wide range of biological activities, such as anticancer [3], anti-inflammatory properties [4], antibacterial [5] and adenosine receptor antagonists [6]. Methylenaminopyrimidine derivatives were synthesized from the reactions of acetophenoncarbazones with various furandione derivatives. N-aminopyrimidine-2-one derivatives (1-3) were synthesized from the hydrolysis of methylenaminopyrimidine derivatives in the acidic medium [7-9]. Aminopyrimidine-2-one derivatives appeared to be an important starting compound in synthetic organic chemistry. In recent years, the reactions of aminopyrimidine-2-one derivatives with anhydrides [10], isothiocyanate [11], 1,3-dicarbonyl compounds [12, 13] and transition metal complexes [14] have been reported. Nowadays, theoretical and experimental comparison of N-aminopyrimidine-2-one derivatives has become popular [15]. Acetylenedicarboxylate derivatives are electron-minus acetylenic molecules having two ester groups. They are prerogative and expedient compounds which engage in easily and practically in heterocyclization [16]. Because of having two ester group, acetylenedicarboxylate derivatives easily undergoes Michael addition that create a chance to synthesize heterocyclic molecules with diverse ring

sizes. The compounds (**1-3**) were made in two steps from furan-2,3-diones and acetophenonsemicarbazone derivatives (**Scheme 1**).

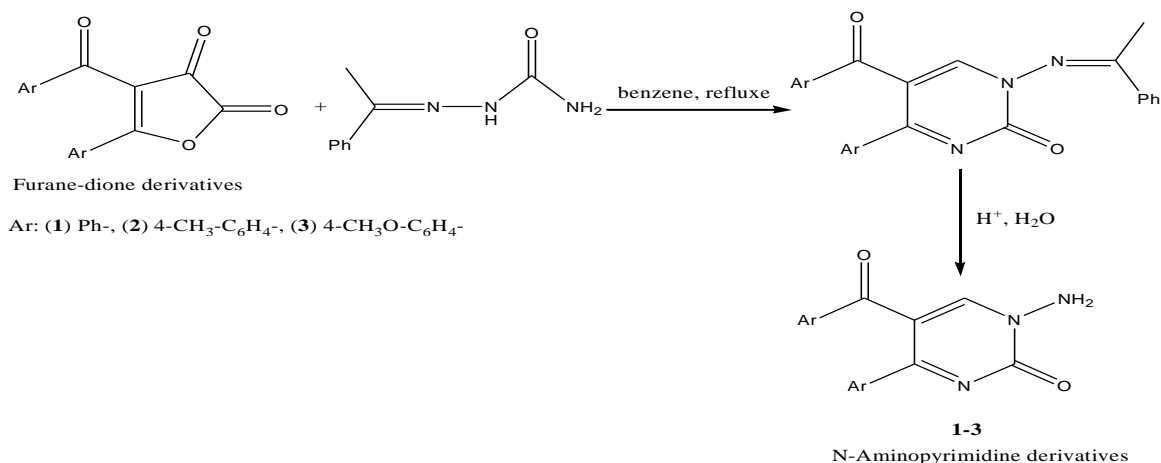
Considering the biological activities of these compounds, in this study, pyrimidin-1(2*H*)-ylaminofumarate derivatives (4-6) were synthesized from the reactions of aminopyrimidine-2-one derivatives (1-3) with dimethyl acetylenedicarboxylate. The synthesized and investigated compounds: dimethyl 2-(5-benzoyl-2-oxo-4-phenylpyrimidin-1(2*H*)-ylamino)fumarate (4), dimethyl 2-(5-(4-methylbenzoyl)-4-(4-methylphenyl)-2-oxopyrimidin-1(2*H*)-ylamino)fumarate (5) and dimethyl 2-(5-(4-methoxybenzoyl)-4-(4-methoxyphenyl)-2-oxopyrimidin-1(2*H*)-ylamino)fumarate (6) are shown in Table 1 [17]. In experimental studies, the structures of molecules were defined by FT-IR, ¹H-NMR and ¹³C-NMR spectroscopies.

Table-1: Structures of investigated compounds.



Compound	R
4	H-
5	CH ₃ -
6	CH ₃ O-

***To whom all correspondence should be addressed.**



Scheme-1: General synthesis reaction of N-aminopyrimidine-2-one derivatives (1-3).

In addition to experimental study, all calculations were done using DFT/B3LYP method. Optimisation of molecules was performed by using 6-311++G(2d,2p) basis set of Gaussian 09, Revision A.02 program [18]. This basis set is known as one of the basic sets that provide more accurate results in determining the electronic and geometric properties for a variety of organic compounds [19]. The quantum chemical calculation of the molecules was carried out using density functional theory/the integral equation formalism polarizable continuum model (DFT/IEFPCM) [20], with basis set 6-311++G(2d,2p) for solvent phase. Quantum chemical parameters for investigated molecules such as; the energy of the highest occupied molecular orbital (E_{HOMO}), the energy of the lowest unoccupied molecular orbital (E_{LUMO}), HOMO-LUMO energy gap (ΔE), ionization potential (I), chemical hardness (η), chemical softness (σ), electronegativity (χ), chemical potential (μ), dipole moment (DM), global electrophilicity (ω) and total of negative Mulliken atomic charges (TMAC), Mulliken charges of some atoms for gas and solvent phase of neutral molecules were calculated. The relationship between the activity and stability of molecules is discussed with the help of these calculated quantum chemical parameters. For example, E_{HOMO} and E_{LUMO} are associated with electron donating capability and electron accepting capability of a molecule; I is one of the basic indicators of chemical reactivity, η and σ are widely used in chemistry to explain the stability of compounds. Recently, the optimization of the molecules by using different basic sets and the discussion of the results has been widely used [21-41]. The experimental and calculated ¹³C and ¹H-NMR spectra results of compounds was discussed.

Experimental

General materials and instruments

Chemicals and all solvents were commercially available and used without further refinement. Melting points were set on the digital melting point apparatus (Electrothermal 9100). The compounds were regularly checked for their homogeneity by Thin Layer Chromatography (TLC) using DC Alufolien Kieselgel 60 F254 (Merck) and Camag TLC lamp (254/366 nm). The IR spectra were recorded on a FT-IR spectrophotometer (Shimadzu Model 8400). The ¹H and ¹³C-NMR spectra were recorded by Bruker 400(100) MHz Ultra Shield instrument. The chemical shifts (δ) are indicated in ppm from tetramethylsilane as a standard.

General procedure for the synthesis of pyrimidin-1(2H)-ylaminofumarate derivatives (4-6)

Compounds (1-3) (1 mmol) and dimethyl acetylenedicarboxylate (1.3 mmol) were refluxed in 30 mL ethanol for 24 hours. The solvent was vaporized. After then the residue was treated with dry diethyl ether and filtered. The raw product was recrystallized from ethanol.

Dimethyl 2-(5-benzoyl-2-oxo-4-phenylpyrimidin-1(2H)-ylamino)fumarate (4)

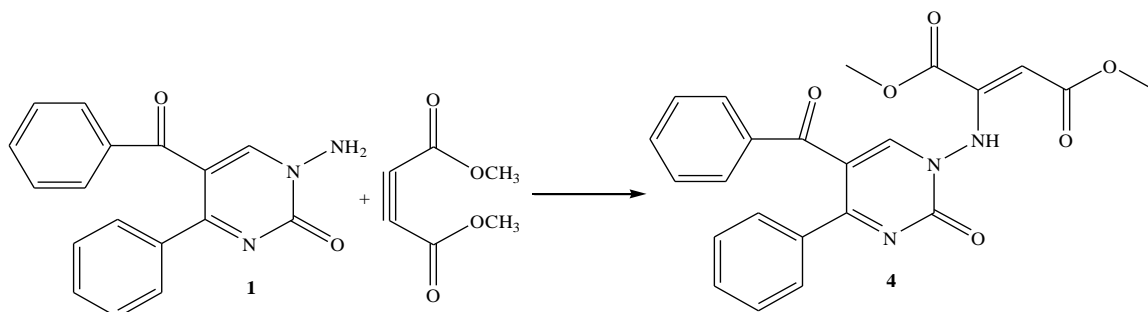
Compound 4 was prepared as a colourless solid from compound 1 and dimethyl acetylenedicarboxylate (Scheme 2). Yield: 68%; m.p.: 232–234 °C. FT-IR ν (cm⁻¹): 3249 (N-H), 3058, 2964 (Ar-C-H and aliphatic C-H), 1750, 1716 (C=O of ester), 1671, 1645 (C=O of pyrimidine ring and benzoyl), 1598, 1574, 1500 (C=N, C=C). Elemental analysis (%)

for $C_{23}H_{19}N_3O_6$, Found (Calc.): C= 63.65 (63.74); H= 4.30 (4.42); N= 9.61 (9.70).

1H -NMR (400 MHz, DMSO): δ (ppm)= 10.24 (s, 1H, pyrimidine -CH), 7.41-7.04 (m, 10H, ArH), 5.61-5.58 (d, 1H, -NH), 4.25-4.21 (d, 1H, =CH), 3.78-3.71 (s, 6H, 2x-OCH₃). ^{13}C -NMR (100 MHz, CDCl₃): δ (ppm)= 194.5, 170.8, 161.4, 147.6, 147.3, 145.8, 139.2, 132.9, 131.9, 130.5, 130.4, 129.3, 128.3, 127.9, 109.6, 65.6, 57.7 and 53.2-53.0 (2x-OCH₃).

Dimethyl 2-(5-(4-methylbenzoyl)-4-(4-methylphenyl)-2-oxypyrimidin-1(2H)-ylamino)fumarate (5)

Compound **5** was prepared as a colourless solid from compound **2** and dimethyl acetylenedicarboxylate (Scheme-3). Yield: 74%; m.p.: 194-196 °C. FT-IR ν (cm⁻¹): 3262 (N-H), 3050, 2950 (Ar-C-H and aliphatic C-H), 1750, 1714 (C=O of ester), 1670, 1644 (C=O of pyrimidine ring and benzoyl), 1597, 1573, 1512 (C \equiv N, C \equiv C). Elemental analysis (%) for $C_{25}H_{23}N_3O_6$, Found (Calc.): C= 64.95 (65.07); H= 4.90 (5.02); N= 9.02 (9.11).



Scheme-2: The reaction for the formation of the **4**.

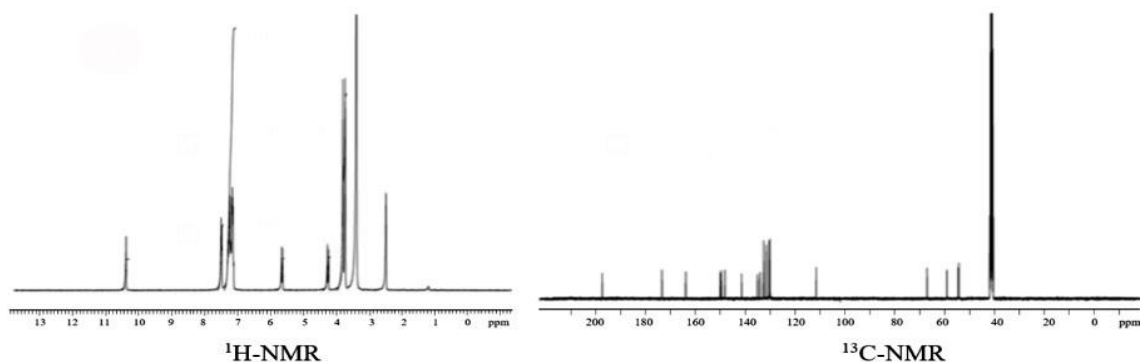
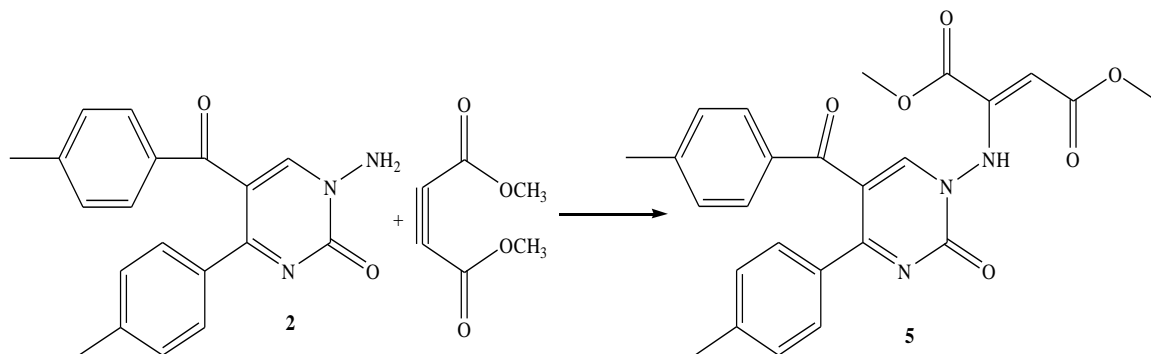
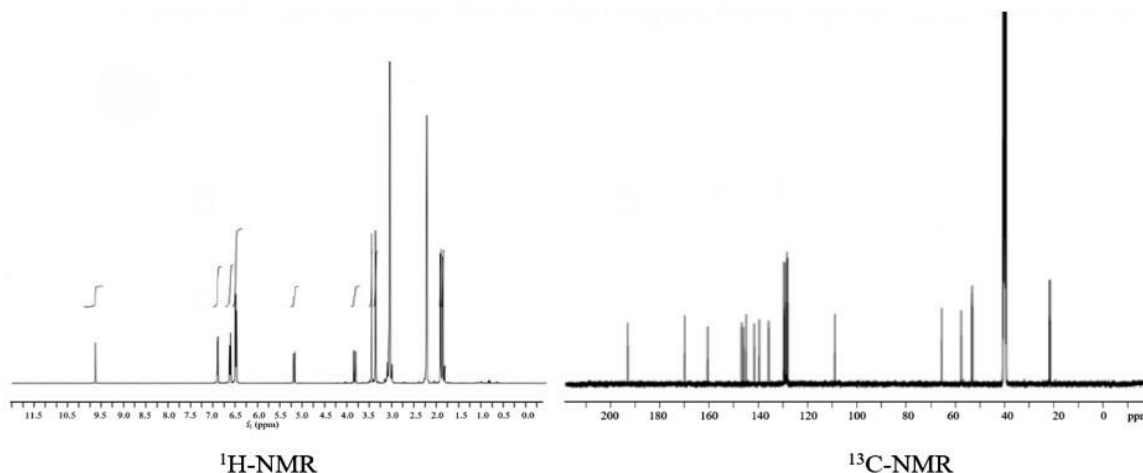


Fig. 1: 1H and ^{13}C -NMR spectra of compound **4**.



Scheme-3: The reaction for the formation of the **5**.

Fig. 2: ^1H and ^{13}C -NMR spectra of compound **5**.

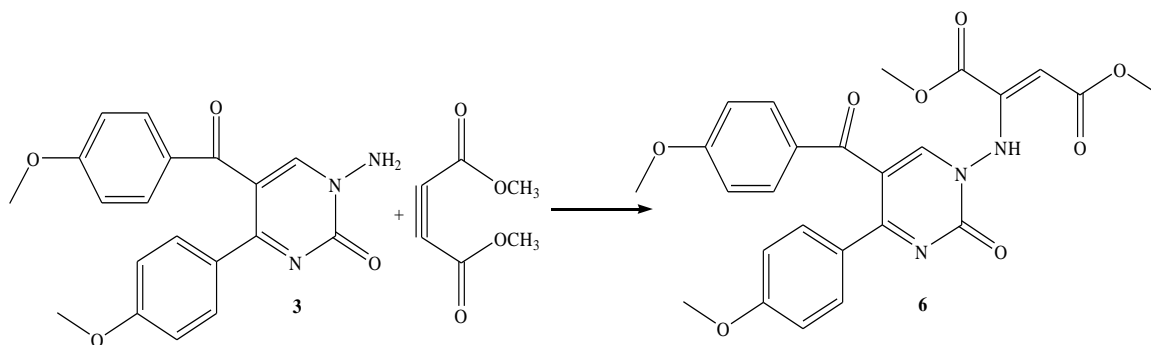
^1H -NMR (400 MHz, DMSO): δ (ppm)= 10.24 (s, 1H, pyrimidine -CH), 7.34-6.90 (m, 8H, ArH), 5.57-5.53 (d, 1H, -NH), 4.17-4.13 (d, 1H, =CH), 3.77-3.66 (s, 6H, 2x-OCH₃), 2.16-2.12 (s, 6H, 2x-CH₃). ^{13}C -NMR (100 MHz, CDCl₃): δ (ppm)= 194.1, 170.7, 161.4, 147.6, 147.5, 146.6, 140.2, 136.4, 130.1, 130.0, 129.5, 129.4, 129.2, 128.8, 128.6, 109.2, 65.5, 57.7, 53.1-53.0 (2X-OCH₃) and 21.4-21.2 (2x-CH₃).

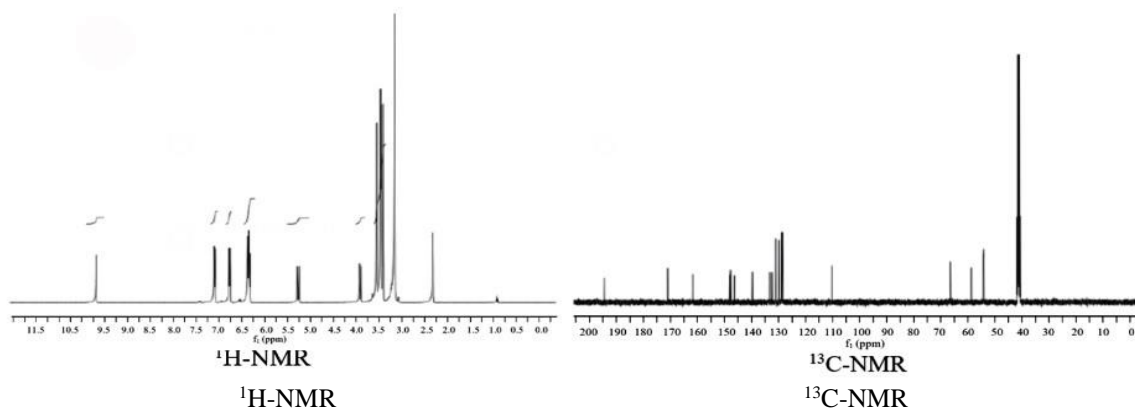
Dimethyl 2-(5-(4-methoxybenzoyl)-4-(4-methoxyphenyl)-2-oxopyrimidin-1(2H)-ylamino)fumarate (**6**)

Compound **6** was prepared as a colourless solid from compound **3** and dimethyl acetylenedicarboxylate (Scheme 4). Yield: 60%; m.p.: 140-142 °C. FT-IR ν (cm⁻¹): 3262.2 (N-H),

3035, 2949 (aromatic and aliphatic C-H), 1750, 1713 (C=O of ester), 1670, 1643 (C=O of pyrimidine ring and benzoyl), 1585, 1575 (C \equiv N, C \equiv C). Elemental analysis (%) for C₂₅H₂₃N₃O₈, Found (Calc.): C= 60.70 (60.65); H= 4.58 (4.70); N= 8.40 (8.52).

^1H -NMR (400 MHz, DMSO): δ (ppm)= 10.40 (s, 1H, pyrimidine -CH), 7.44-6.60 (m, 8H, ArH), 5.54-5.50 (d, 1H, -NH), 4.20-4.17 (d, 1H, =CH), 3.70-3.62 (s, 12H, 4x-OCH₃). ^{13}C -NMR (100 MHz, CDCl₃): δ (ppm)= 194.1, 170.7, 161.4, 147.6, 147.5, 146.6, 140.2, 136.4, 130.1, 130.0, 129.5, 129.4, 129.2, 128.8, 128.6, 109.2, 65.5, 57.7 and 55.60-53.0 (4X-OCH₃).

Scheme-4: The reaction for the formation of the **6**.

Fig. 3: ^1H and ^{13}C -NMR spectra of compound **6**.

Computational details

Molecular properties, based on the reactivity and selectivity of the compounds, were according to the Koopmans' theorem [42] relating of E_{HOMO} and E_{LUMO} . Consistent with the DFT Koopmans' theorem [42, 43], the ionization potential (I) can be estimated as the negative value of E_{HOMO} , such as shown in equation 1:

$$I = -E_{\text{HOMO}} \quad (1)$$

The negative value of E_{LUMO} is similarly related to the electron affinity (A) [44] in equation 2:

$$A = -E_{\text{LUMO}} \quad (2)$$

Energy gap (ΔE) is estimated by using E_{HOMO} and E_{LUMO} :

$$\Delta E = E_{\text{LUMO}} - E_{\text{HOMO}} \quad (3)$$

Electronegativity (χ) is estimated using following the equation from I and A [45, 46]:

$$\chi = \left(\frac{I + A}{2} \right) \quad (4)$$

Chemical hardness (η) calculates the resistance of an atom to a charge transfer [45], it's estimated by using the equation from I and A [46]:

$$\eta = \left(\frac{I - A}{2} \right) \quad (5)$$

Electron polarizability is called chemical softness (σ), relates the capacity of an atom or group of atoms to receive electrons [45] and it is estimated from chemical hardness or E_{HOMO} and E_{LUMO} by using the equation:

$$\sigma = \frac{1}{\eta} \cong - \left(\frac{2}{E_{\text{HOMO}} - E_{\text{LUMO}}} \right) \quad (6)$$

Chemical potential (μ) and electronegativity (χ) can be calculated using the following equations [19] from E_{HOMO} and E_{LUMO} :

$$\mu = -\chi \cong \left(\frac{E_{\text{HOMO}} + E_{\text{LUMO}}}{2} \right) \quad (7)$$

The global electrophilicity index (ω) is a useful reactivity descriptor that can be used to compare the electron-donating capabilities of molecules [47]. A high value of electrophilicity describes a good electrophile while a low value of electrophilicity describes a good nucleophile [48]. The global electrophilicity index is estimated by the equation using the parameters of electronegativity and chemical hardness:

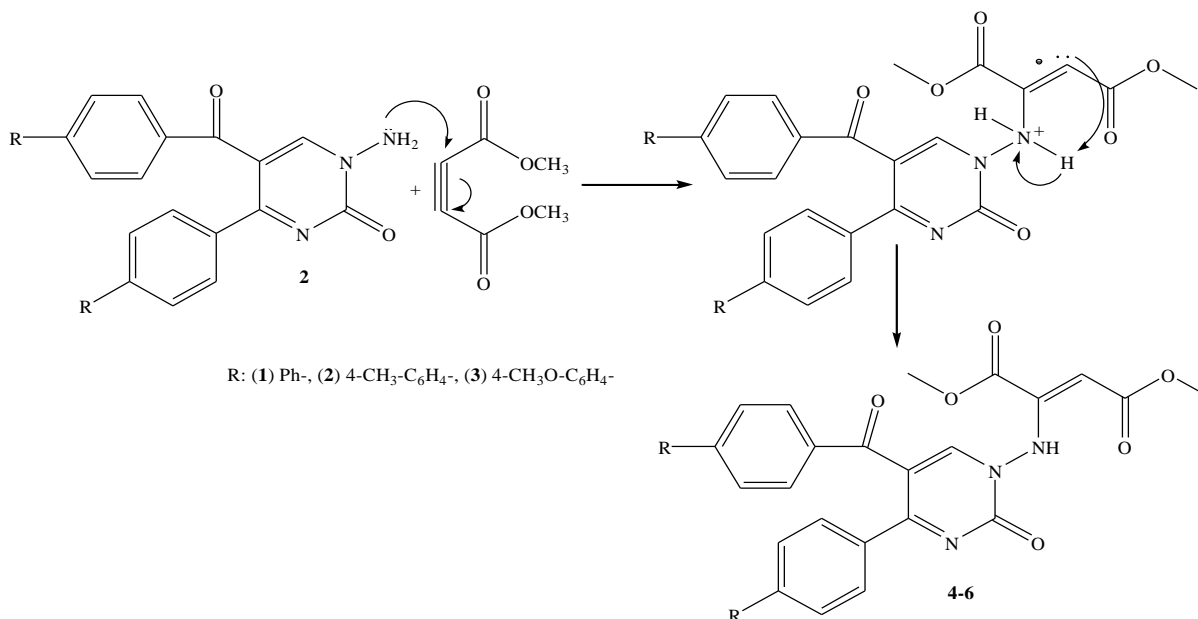
$$\omega = \frac{\chi^2}{2\eta} \quad (8)$$

In addition to those calculated above, the ^1H and ^{13}C -NMR chemical shifts and molecular electrostatic potential (MEP) surface of molecules were found by using by using B3LYP/6-311++G(2d,2p) basic set.

Results and discussion

Structural analysis

The N-aminopyrimidine derivatives (1-3) were prepared as shown in Scheme 1. The new pyrimidin-1(2*H*)-ylaminofumarate derivatives (4-6) were prepared in moderate yields (60-74%) from the reactions of dimethyl acetylenedicarboxylate with 1-3 compounds in Schemes 2-4. All compounds readily purified by recrystallization. The proposed mechanism for the formation of compounds (4-6) is depicted in Scheme 5.



Scheme-5: The mechanism for the formation of the products (4-6).

On treatment of dimethyl acetylenedicarboxylate with N-aminopyrimidine-2-one derivatives (1-3), the reaction should begin by a nucleophilic attack of the nitrogen atom lone pair electrons of N-aminopyrimidine-2-one derivatives (1-3) to the alkyne carbon of dimethyl acetylenedicarboxylate and commence a Michael addition [16]. The structures of the compounds (4-6) were verified by IR, ¹H-NMR and ¹³C-NMR spectra. The details of the reaction pathway of (4-6) with dimethyl acetylenedicarboxylate as outlined are given in Scheme 5

The compound 4 was obtained from the reaction of compound 1 and dimethyl acetylenedicarboxylate in 68% yield. The IR spectrum of compound 4 showed the presence of NH group at 3249 cm⁻¹. The IR spectrum of compound 4 showed significant characteristic stretching bands to the C=O groups. These bands were observed at 1750, 1716, 1671 and 1645 cm⁻¹. In the ¹H-NMR spectrum, NH proton in the structure of compound 4, resonated at 5.61-5.58 ppm. The aromatic protons of 4 were observed in the 7.41-7.04 ppm as multiplet. The signals of methoxy protons in the structure of 4 were observed at 3.78 and 3.71 ppm as singlets. ¹³C-NMR spectra showed highest frequency signal observed at 194.5 ppm to the benzoyl carbon. The signals of CH₃O- groups were observed at 53.2, 53.0 ppm and other carbons were determined in the 170.8-57.7 ppm region. The results of measurement of 5 and 6 compounds were given in the experimental section.

Molecular structure

E_{HOMO}, E_{LUMO}, ΔE, I, η, σ, χ, etc. values were calculated for the pyrimidin-1(2H)-ylaminofumarate derivatives (after that, it will be called as briefly pyrimidine derivatives or 4-6) with the DFT/B3LYP/6-311++G(2d,2p) method for gas and solvent (ethanol) phase of neutral molecules, as shown in Figs. 4-7, and Tables 2-6.

On the authority of the frontier molecular orbital (FMO) theory, the chemical reactivity of molecule is a function of interaction between HOMO and LUMO levels of the reacting species [49]. HOMO and LUMO are known as frontier orbitals, and these a molecule play important role in the determination of its molecular reactivity or stability. Some researchers mention that FMO theory is useful in anticipating the molecule's interaction center [50-52]. The FMOs (HOMOs, LUMOs) of molecules are given in Fig. 4. It could be easily found that the HOMO distributions of 4 and 5 compounds for gas phase are mainly located around of pyrimidine ring, amine and carbonyl groups. Fig. 4 shows that the HOMO distributions for in the solvent phase of compound 4 are approximately the same, the distribution in compound 5 appears to be predominantly on the 4-methyl-phenyl groups. In compound 6 it can be seen that the HOMO distributions for both phases are above the 4-methyl-phenyl groups. The electron-rich regions of the molecule can be said to be more active. The presence of nitrogen and oxygen atoms on these molecules to

be causes strong activity. Also, this figure shows that there is much more electron density in nitrogen and oxygen atoms of 4 and 5 compounds, and methoxy groups of compound 6. The results show that interaction of molecules with this groups bond in 4-6 is easier.

It is important to note that the most effective corrosion inhibitors are π -systems and heterocyclic organic compounds including heteroatoms such as O, N, S [53]. This situation indicates that these compounds can also be used as a corrosion inhibitor. Corrosion inhibition process can be described as the formation of donor-acceptor surface complexes between vacant d -orbital of a metal with free or π -electrons of organic inhibitor, generally including aforementioned heteroatoms [54]. The LUMO distributions of 4-6 molecules are mainly located around of the pyrimidine and non-carbonyl phenyl ring for both phases. The charge density distribution

of HOMO and LUMO level of compounds 4-6 for gas and solvent phase are shown in Fig. 4.

On the authority of FMO, E_{HOMO} and E_{LUMO} are associated with electron donating capability and electron accepting capability of a molecule. High E_{HOMO} is essential for reaction with nucleophiles of molecule while low E_{LUMO} is essential for reaction with electrophiles [55]. E_{HOMO} values were found in gas phase for 4-6 molecules -6.791, -6.680, -6.430 eV for gas phase, and -7.079, -6.941, -6.508 eV for solvent phase, respectively (Fig. 5).

According to these results, the sequence of reactivity for gas phase of study molecules can be written as: 6>5>4 for gas and solvent phase. E_{HOMO} values in molecule 6 is lower than other molecules as negative. This condition is due to the methoxy group attached to the phenyl ring of 6 molecules. As is known, the methoxy group is an electron attracting group.

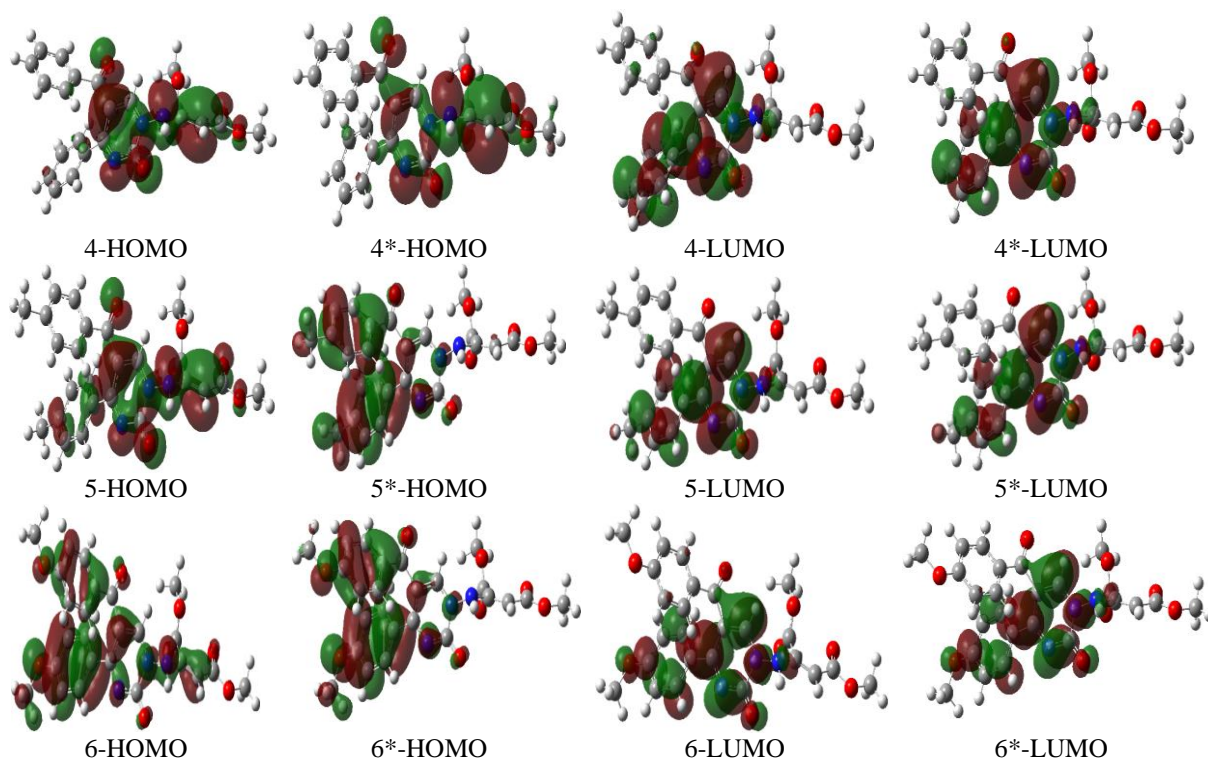


Fig. 4: The frontier MOs (HOMOs, LUMOs) molecules by using DFT/B3LYP/6-311++G(2d,2p) basic set for gas and ethanol (*) phase.

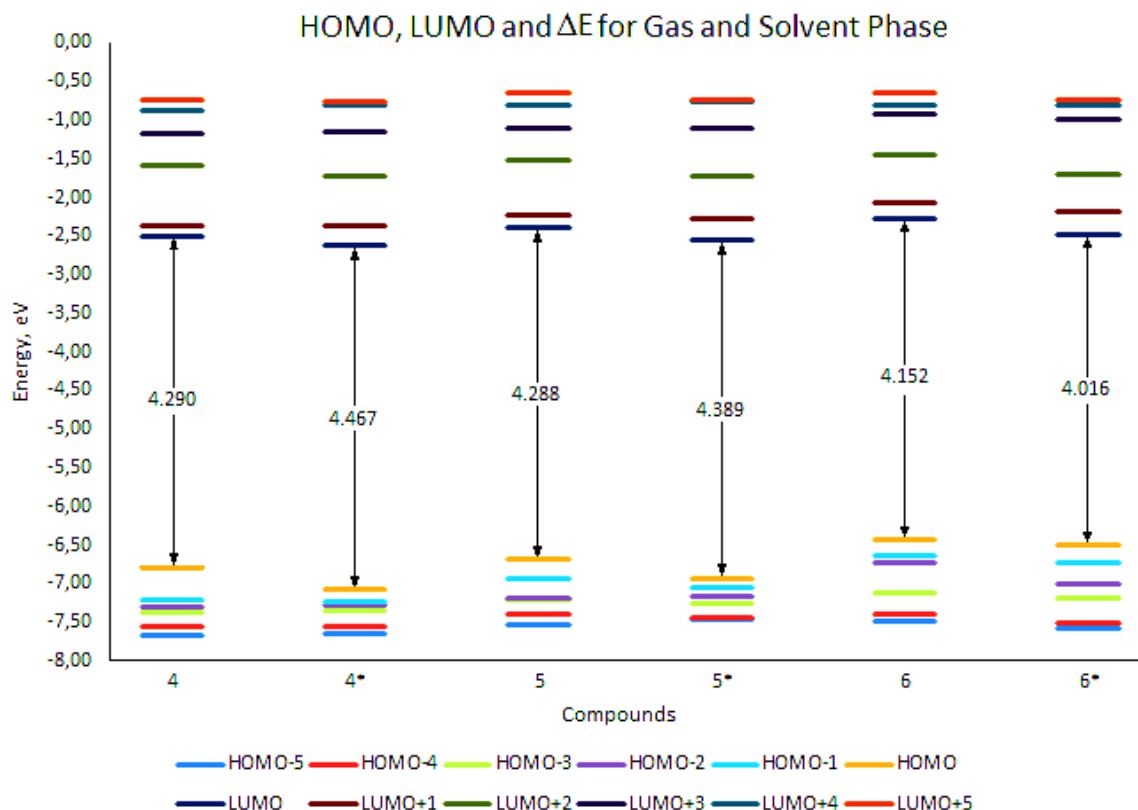


Fig. 5: The calculated HOMO, LUMO and energy gap (ΔE) parameters for gas and solvent (*: ethanol) phase of neutral molecules using B3LYP/6-311++G(2d,2p) method.

HOMO-LUMO energy gap (ΔE , see eq. 3), chemical hardness and softness are closely related to chemical properties [56-60]. Chemical hardness introduced in 1960s by Pearson [53] is defined as the resistance to electron cloud polarization or chemical species deformation. On the authority of the Maximum Hardness Principle states; “a chemical system tends to arrange itself so as to achieve maximum hardness and chemical hardness can be considered as a measurement of stability” [61].

The physical properties of the compounds are highly dependent on ΔE between the compounds. The large ΔE indicates a high kinetic stability and also low molecular activity of the compound. Because, the higher ΔE of the molecules are difficult to polarize. The compounds require more energy to excite, but smaller energy gaps are relatively easy to polarize and react more efficiently than higher energy gaps. Pearson showed that hard molecules with a high ΔE values are more stable compared to soft molecules with a low ΔE values [62, 63]. The smaller ΔE is often interpreted by a stronger activity and perhaps greater inhibition efficiency [50]. So, ΔE decreases, the reactivity of the molecule increases

leading to a better inhibition efficiency and activity [60].

ΔE values for gas phase were found 4.290, 4.288, 4.152 eV of 4-6 molecules and 4.467, 4.389, 4.016 eV for solvent phase of 4-6 molecules, respectively. ΔE values in the gas phase are lower than the solvent phase for 4-6 molecules. Therefore, the gas phase is expected to be more active than solvent phase. It can be seen that the ΔE values of molecules 4 and 5 are very close to each other for gas phase. It is seen that the ΔE value of molecule 6 is slightly lower for both phases. In this case, molecule 6 is found more active than other molecules for gas and solvent phase due to the fact that a low ΔE value is observed (Fig. 5). It appears that the most active compound is 6 for gas and solvent phase.

Ionization potential (I) is one of the basic indicators of chemical reactivity. High values of the ionization potential (Eq. 1) demonstrate the chemical inertness and strong stability, while low ionization energy indicates high activity of the atoms and molecules [59]. According to ionization potential values, order of activity can be written as: **6** (6.430

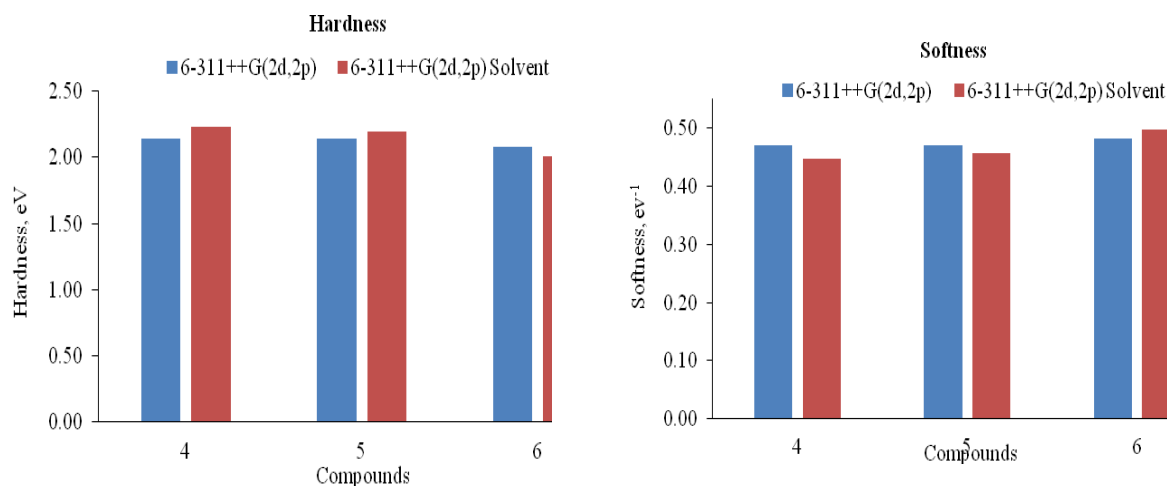
eV)<5 (6.680 eV)<4 (6.791 eV) for gas phase and 6 (6.508 eV)<5 (6.941 eV)<4 (7.079 eV) for solvent phase. As in ΔE values, in the gas phase I values are lower than the solvent phase for 4-6 molecules. Molecule 6 is found more active than other molecules for gas and solvent phase. Because, molecule 6 has the lowest ionization potential values. It can be seen from results that the stable for gas and water phase belongs to molecule 4.

The hardness (η) and softness (σ) are widely used in chemistry to explain the stability of compounds. On the authority of the Maximum Hardness Principle [53], chemical hardness is a rate of the stability of chemical species. The hardness (see eq. 5) is just half the energy gap between the E_{HOMO} and E_{LUMO} . If a molecule has a large energy gap, it is called hard and other wise is called soft. The active compounds have a greater softness value. Softness (see eq. 6) is a quantity of the polarizability. Soft molecules give more easily electrons to an electron acceptor molecule or surface [19]. The calculated chemical hardness and softness values are given in Fig. 6.

According to softness values, electron donating trend of studied chemical compounds may be written as: $6 > 5 \approx 4$ for gas phase, and $6 > 5 > 4$ for solvent phase. The softness values for gas phase were found 0.466, 0.466, 0.482 eV of 4-6 molecules and 0.448, 0.456, 0.498 eV for solvent phase of 4-6 molecules, respectively. Molecule 6 was found the most active molecule for gas and solvent phases.

The average values of the E_{HOMO} and E_{LUMO} have been defined as the chemical potential (μ). The negative value of the chemical potential was called electronegativity (χ) (see eq. 4). Chemical potential, electronegativity and hardness are descriptors for the predictions about chemical properties of molecules [64]. Electronegativity also indicates the tendency of an inhibitor molecule. Electronegativity is which represents the attraction of the electrons [19]. In general, a molecule with lower electronegativity is associated with a higher electron donor bias and therefore exhibited a higher activity compared to a molecule with a higher electronegativity value [65]. The electronegativity (χ) values were found 4.646, 4.536, 4.354 for gas phase and 4.846, 4.746, 4.500 eV for solvent phase of 4-6 molecules, respectively. The electronegativity value of 6 is more active than other molecules for both phases (see Fig. 6).

Dipole moment (DM) is another indicator of activity of chemical compounds. Although some authors reported that there is no notable relationship between dipole moment and inhibition efficiency [57, 66] and some authors showed that activity increases with the increasing dipole moment [67-69]. In some studies, authors supported that increasing value of dipole moment facilitates the electron-transport process [68, 69]. For instance, in Table 2, calculated dipole moment values for 4-6 molecules are 4.625, 5.714, 6.918 for gas phase and 8.278, 9.525, 10.868 Debye for solvent phase, respectively (Table 2). According to dipole moment results, molecule 6 was found to be the best active for gas and solvent phase.



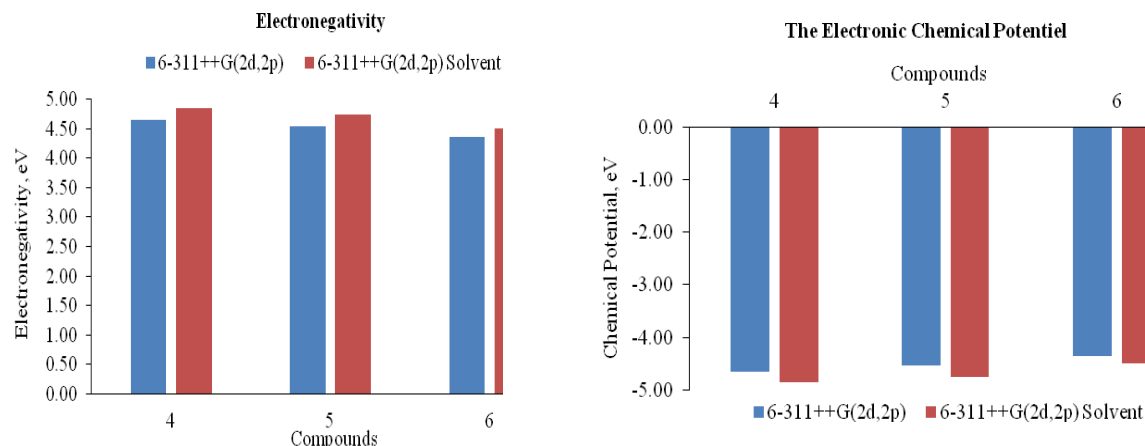


Fig. 6: The calculated some quantum chemical parameters for gas and solvent phase compounds using B3LYP/6-311++G(2d,2p) method (solvent: ethanol).

The total of negative Mulliken atomic charges (TMAC) can be seen from Table 2. The TMAC values have been found as: 4 (-3.626 eV), 5 (-4.141 eV), 6 (-3.481 eV) for gas phase and 4 (-3.932 eV), 5 (-4.402 eV), 6 (-3.652 eV) for solvent phase. According to dipole moment results, 5 were found as the best active molecule for both phases. The negative charge densities have been shown to increase on active molecules. This result is the different as of the order of activity of molecules found by other calculation methods for gas and solvent phase. In other methods, molecule 6 has been found as the most active compound for both phases. The results of other calculations: global electrophilicity index (ω) and MV can be seen in Table 2.

Table-2: The calculated some quantum chemical parameters for gas and solvent phase of the neutral compounds using B3LYP/6-311++G(2d,2p) method.

Molecule	I, eV	DM, Debye	MV, cm ³ /mol	TMAC, e	ω , eV
4	6.791	4.625	298.294	-3.626	5.031
5	6.680	5.714	342.787	-4.141	4.798
6	6.430	6.918	334.346	-3.481	4.565
4*	7.079	8.278	286.620	-3.932	5.257
5*	6.941	9.525	315.922	-4.402	5.132
6*	6.508	10.868	318.322	-3.652	5.043

*Solvent phase: Ethanol

DFT study can be used to better understand the molecular behaviour and structural conformation of the compounds. DFT approach helps to study the electrostatic potential (ESP) distribution of the

compound more precisely. Molecular Electrostatic Potential (MEP) is used to describe the electrostatic interaction between a molecule and an atom. ESP is indicating the electrophilic and nucleophilic nature of the molecules, and its essential tools to study the reactivity nature of the compounds. ESP surfaces of the compounds are shown from Fig. 7.

MEP maps at the surface are represented by different colours. The blue colour in the ESP graphs represents the maximum amount of the positive region in which the nucleophilic reaction takes place, and the reddish region represents the negative region in which the electrophilic reaction occurs [62], and green colour represents zero potential [70].

Fig. 7 shows that the electron density increases around the oxygen atoms with the negative electrostatic potential values of the molecules. Especially, most of the electrophilic reactions takes place of carbonyl oxygen of the pyrimidine ring (7O), O45 and O46 oxygen atoms (the numbers of oxygen atoms can be seen from the figure in Table-3) for gas and solvent phase of all compounds, and the red coloured region in Fig. 7 shows the maximum electronegativity. This result indicates that these atoms will enter the electrophilic reactions more easily. On the other hand, it can be seen that the electron density decreases around 5N and 8N atoms with the positive electrostatic potential values of the compounds.

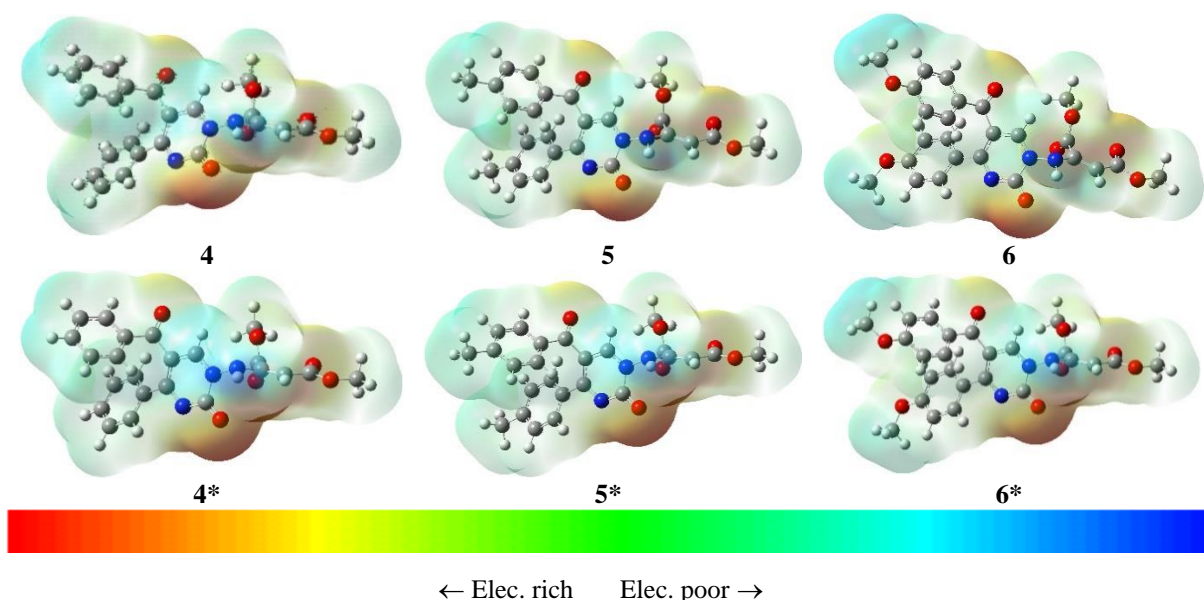
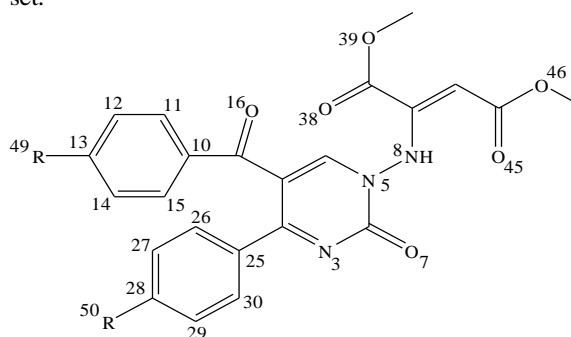


Fig. 7: Molecular electrostatic potential (MEP) surface of molecules by using DFT/B3LYP/6-311++G(2d,2p) basic set for gas and ethanol (*) phase.

In such studies, electronic charge analysis for atoms in the molecules is important because binding ability of a molecule also depends on the electronic charge on heteroatoms of the molecule. The binding facilitates as the negative charge on hetero atom increases [71]. In this study, we used Mulliken population analysis to calculate the atomic charges [72]. Mulliken atomic charges on nitrogen, oxygen and carbon atoms of phenyl rings of molecules 4-6 for non-protonated gas and solvent phase are given in Table 3. As can be seen from Table 3, the negative charge densities are more on 7, 45, 46, 49 and 50 number oxygen atoms from other oxygen, nitrogen and carbon atoms. It is seen that oxygen atoms with high Mulliken charges are electron rich in ESP graphs. It is seen that the charge of carbon atoms in the phenyl rings according to the atoms and groups bound in the molecules 4-6 is changing. It is seen from Table 3 that, while the charge of 14, 15, 26 and 27 number carbon atoms are increased in molecule 5 to which the electron donor methyl group is attached, Mulliken charges of the carbon atom in molecule 6 to which the electron-attracting methoxy group is bound generally decreases. The Mulliken negative charges values are generally lower in gas phase than in solvent phase for all compounds. It is easier to bind a molecule from these negative charge atoms where the negative value is higher. As a result, these atoms in molecules to be causes strong interaction.

Table-3: Calculated Mulliken atomic charges (e) on nitrogen, oxygen and carbon atoms of phenyl rings of 4-6 compounds by using B3LYP/6-311++G(2d,2p) basic set.

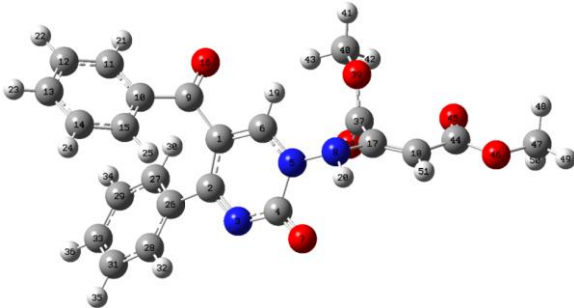


Atom	4	5	6	4*	5*	6*
3N	-0.360	-0.365	-0.385	-0.420	-0.417	-0.431
5N	0.078	0.094	0.100	0.059	0.080	0.101
7O	-0.461	-0.466	-0.469	-0.523	-0.529	-0.536
8N	-0.204	-0.202	-0.204	-0.195	-0.236	-0.243
10C	0.217	0.311	0.211	0.332	0.361	0.277
11C	0.034	-0.073	-0.108	0.083	-0.059	-0.094
12C	-0.345	-0.135	-0.158	-0.390	-0.177	-0.144
13C	-0.178	0.299	-0.030	-0.212	0.272	-0.019
14C	-0.146	-0.466	-0.096	-0.191	-0.497	-0.155
15C	-0.384	-0.469	-0.185	-0.447	-0.482	-0.265
25C	0.491	0.584	0.523	0.453	0.495	0.478
26C	-0.221	-0.419	-0.215	-0.260	-0.408	-0.322
27C	-0.229	-0.471	-0.107	-0.279	-0.428	-0.171
28C	-0.230	0.188	-0.084	-0.263	0.272	-0.061
29C	-0.297	-0.156	-0.171	-0.319	-0.291	-0.165
30C	-0.132	-0.070	-0.204	-0.151	-0.150	-0.197
16O	-0.411	-0.419	-0.433	-0.466	-0.475	-0.494
38O	-0.292	-0.290	-0.291	-0.363	-0.364	-0.365
39O	-0.202	-0.198	-0.198	-0.190	-0.190	-0.191
45O	-0.461	-0.462	-0.462	-0.532	-0.532	-0.533
46O	-0.423	-0.423	-0.424	-0.439	-0.439	-0.439
49O	-	-	-0.426	-	-	-0.452
50O	-	-	-0.426	-	-	-0.451

*Ethanol phase

We calculated the ^1H and ^{13}C -NMR chemical shifts by using Gaussian 09, Revision A.02 program [18]. The ^1H and ^{13}C -NMR results calculated by using B3LYP/6-311++G(2d,2p) basic set are shown in Tables 4-6 for the pyrimidin-1(2*H*)-ylamino)fumarate derivatives. The experimental and calculated ^1H and ^{13}C -NMR chemical shifts results are given comparatively in these tables. Since the signals of the carbon and hydrogen atoms in the pyrimidine and the phenyl ring overlap too much, they are given as the range in results of these tables. In addition, the hydrogen atoms of methyl, methoxy and naphthyl groups are also given as the range because of overlap.

Table-4: Experimental and calculated with B3LYP/6-311++G(2d,2p) basic set results of ^{13}C and ^1H -NMR as ppm for molecule 4.

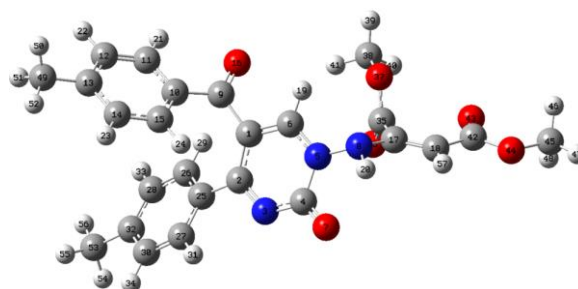


Atom	Experimental	Calculated	Atom	Experimental	Calculated
1C		124.4	19H	10.24	8.61
2C		178.9	20H	5.61-5.58	8.29
4C	147.6	157.9	21H	7.41-7.04	8.63
6C		155.9	22H		7.91
9C	194.5	200.7	23H		7.80
10C	170.8-57.7	143.7	24H		7.44
11C		137.0	25H		7.64
12C		134.2	30H		7.66
13C		139.2	32H		8.71
14C		132.8	34H		7.52
15C		138.0	35H		7.78
26C		145.7	36H		7.74
27C		137.0	41H	3.78-3.71	4.08
28C		137.5	42H		4.41
29C		133.5	43H		4.46
31C		134.7	48H		3.99
33C		137.7	49H		3.65
17C		163.3	50H		3.99
18C		102.2	51H	4.25-4.21	5.79
44C		173.8			
40C	53.0	54.7			
37C		171.1			
47C	53.2	57.1			

According to the data given in Tables 4-6, the ^{13}C chemical shifts for the carbon atoms of the carbonyl group (9C) of 4-6 molecules have been recorded in the range 194.5 ppm, and they are calculated as 200.7-199.2 ppm. Similarly, the methoxy groups of 4-6 compounds were observed as 53.0-53.7, 53.1-53.0, 53.1-53.0 ppm and calculated as 54.7-57.1, 57.0-54, 57.0-54.6 ppm, respectively

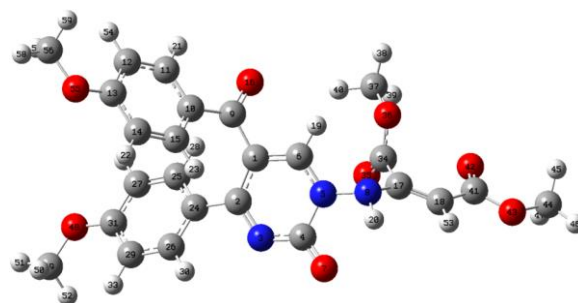
and the methyl groups of 5 compound were observed as 21.4-21.2 ppm and calculated as 23.8 ppm. ^1H -NMR chemical shifts for the NH of 4-6 compounds have been recorded in the range 5.61-5.58, 5.57-5.33 and 5.54-5.50 ppm, respectively, whereas the corresponding shifts have been simulated at 8.29-8.25 ppm at B3LYP level for the NH. It is seen the other results from Tables 4-6 that the experimental and calculated results are generally compatible.

Table-5: Experimental and calculated by B3LYP results of ^{13}C and ^1H -NMR as ppm for molecule 5.



Atom	Experimental	Calculated	Atom	Experimental	Calculated
1C		125.1	19H	10.24	8.62
2C		178.1	20H	5.57-5.33	8.28
4C		157.7	21H	7.34-6.90	8.71
6C		156.5	22H		7.49
9C	194.5	200.4	23H		7.31
10C		142.7	24H		7.39
11C		137.6	29H		7.66
12C		137.0	31H		8.63
13C		152.5	33H		7.20
14C		133.6	34H		7.69
15C		137.5	39H	3.77-3.66	4.08
25C		143.1	40H		4.46
26C		137.5	41H		4.57
27C		137.4	46H		3.97
28C		134.0	47H		3.69
30C		135.6	48H		3.97
32C		150.9	57H	4.17-4.13	5.76
17C		163.2	50H	2.16-2.12	2.81
18C		101.6	51H		2.64
42C		173.9	52H		2.22
35C		171.0	54H		2.77
38C	53.1-53.0	57.0	55H		2.56
45C		54.7	56H		2.09
49C	21.4	23.8			
53C	21.2	23.8			

Table-6: Experimental and calculated by B3LYP results of ^{13}C and ^1H -NMR as ppm for molecule 6.



Atom	Experimental	Calculated	Atom	Experimental	Calculated
1C		124.8	19H	10.40	8.57
2C		176.9	20H	5.54-5.50	8.25
4C		157.6	21H	7.44-6.60	8.83
6C		156.4	22H		6.95
9C	194.5	199.2	23H		7.46
10C		137.0	54H		7.10
11C		139.6	28H		7.62
12C		114.3	30H		8.76
13C		172.0	32H		6.94
14C		121.5	33H		7.15
15C		140.0	53H	4.20-4.17	5.74
24C		137.4	38H	3.70-3.62	4.06
25C		139.2	39H		4.48
26C		140.4	40H		4.55
27C		122.3	45H		3.96
29C		114.0	46H		3.67
31C		171.4	47H		3.96
17C		163.4	50H		3.78
18C		101.2	51H		4.23
34C		171.0	52H		3.81
41C		173.9	57H		3.78
37C	55.60-53.0	57.0	58H		4.18
44C		54.6	59H		3.83
49C		55.9			
56C		56.6			

Conclusions

A series of the pyrimidin-1(2H)-ylaminofumarate derivatives (4-6) were synthesized, and their ¹H-NMR, ¹³C-NMR and elemental analysis were performed. The quantum chemical parameters of the synthesized pyrimidin-1(2H)-ylaminofumarate derivatives have been found and discussed. According to found results, 6 is found the most active molecule than 4 and 5 for gas and solvent phase of neutral compounds. Mulliken charge high oxygen atoms were found to be electron rich in ESP graphs for notr and solvent phase. Most of the electrophilic reactions were found to be the carbonyl oxygen of the pyrimidine ring (7O), O45 and O46 oxygen atoms for the gas and solvent phases of all compounds. The experimental and calculated NMR results of compounds were found generally compatible.

Acknowledgement

The experimental part of this study was presented by Kokbudak and at al. as full text in *2nd International Scientific and Vocational Studies Congress*, and the computers allocated by the Erciyes University data center were used for quantum chemical calculations.

References

1. D. H. Boschelli, Z. Wu, S. R. Klutchko, H. D. H. Showalter, J. M. Hamby, G. H. Lu, T. C. Major, T. K. Dahring, B. Batley, R. L. Panek, J. Keiser, B. G. Hartl, A. J. Kraker, W. D. Klohs, B. J. Roberts, S. Patmore, W. L. Elliott, R. Steinkampf, L. A. Bradford, H. Hallak and A. M. Doherty, Synthesis and tyrosine kinase inhibitory activity of a series of 2-amino-8H-pyrido[2,3-d]pyrimidines: identification of potent, selective platelet-derived growth factor receptor tyrosine kinase inhibitors, *J. Med. Chem.*, **41**, 4365 (1998).
2. S. R. Walker, E. J. Carter, B. C. Huff and J. C. Morris, Variolins and related alkaloids, *Chem. Rev.*, **109**, 3080 (2009).
3. H. Shao, S. Shi, S. Huang, A. J. Hole, A. Y. Abbas, S. Baumli, X. Liu, F. Lam, D. W. Foley, P. M. Fischer, M. Noble, J. A. Endicott, C. Pepper and S. Wang, Substituted 4-(thiazol-5-yl)-2-(phenylamino)pyrimidines are highly active CDK9 inhibitors: synthesis, X-ray crystal structures, structure-activity relationship, and anticancer activities, *J. Med. Chem.*, **56**, 640 (2013).
4. A. R. El-Gazzar and H. N. Hafez, Synthesis of 4-substituted pyrido[2,3-d]pyrimidin- 4(1H)-one as analgesic and anti-inflammatory agents, *Bioorg. Med. Chem. Lett.*, **19**, 3392 (2009).
5. B. L. Narayana, A. R. R. Rao and P. S. Rao, Synthesis of new 2-substituted pyrido[2,3-d]pyrimidin-4(1H)-ones and their antibacterial activity, *Eur. J. Med. Chem.*, **44**, 1369 (2009).
6. S. Federico, A. Ciancetta, N. Porta, S. Redenti, G. Pastorin, B. Cacciari, K. N. Klotz, S. Moro and G. Spalluto, Scaffold decoration at positions 5 and 8 of 1,2,4-triazolo[1,5-c]pyrimidines to explore the antagonist profiling on adenosine receptors: A preliminary structure-activity relationship study, *J. Med. Chem.*, **57**, 6201 (2014).
7. G. Kollenz, Über Reaktionen mit cyclischen Oxalylverbindungen, *Monatshefte. Chem.*, **103**, 947 (1972).
8. B. Altural and G. Kollenz, Reaktions of cyclic oxalyl compounds, part 30 [1]: some reactions with n- amino-pyrimidine derivatives, *Monatshefte. Chem.*, **121**, 677 (1998).
9. Z. Önal and İ. Yıldırım, Reactions of 4-(4-methylbenzoyl)-5-(4-methylphenyl)-2.3-furandione with semi-thiosemi-carbazones, *Heterocycl. Commun.*, **13**, 113 (2007)
10. Z. Önal and B. Altural, Reactions of 1-amino-5-benzoyl-4-phenyl-1H-pyrimidine-2-thione with various carboxylic anhydrides, *Asian J. Chem.*, **18**, 1061 (2006).
11. Z. Önal and A. C. Daylan, Reactions of 1-amino-5-benzoyl-4-phenyl-1H-pyrimidine derivatives with various isothiocyanates, *Asian J. Chem.*, **19**, 2647 (2007).
12. Z. Önal and B. Altural, Reactions of N-aminopyrimidine derivatives. with 1.3-dicarbonyl compounds, *Turk. J. Chem.*, **23**, 401 (1999).

13. Z. Önal, H. Ceran and E. Şahin, Synthesis of novel dihydropyrazolo [1,5-c] pyrimidin-7 (3H)-one/-thione derivatives, *Heterocycl. Commun.*, **14**, 245 (2008).
14. G. Aslan and Z. Önal, Novel metal complexes, their spectrophotometric and QSAR studies, *Med. Chem. Res.*, **23**, 2596 (2014).
15. M. Saracoglu, F. Kandemirli, A. Ozalp and Z. Kokbudak, Synthesis and quantum chemical calculations of 2,4-dioxopentanoic acid derivatives-Part I, *Chem. Sci. Rev. Lett.*, **6**, 1 (2017).
16. W. M. Shu, K. L. Zheng, J. R. Ma and A. X. Wu, Transition-metal-free multicomponent benzannulation reactions for the construction of polysubstituted benzene derivatives, *Org. Lett.*, **17**, 5216 (2015).
17. Z. Kokbudak, S. Buran, Ş. D. Doğan, H. G. Aslan and S. Akkoc, The cytotoxic activity properties and reactions of aminopyrimidine derivatives with dimethyl acetylenedicarboxylate, *2nd Int. Sci. Voc. Stu. Cong., Nevsehir, Turkey*, 330 (2018).
18. M. J. Frisch, G. W. Trucks, H. B. Schlegel, G. E. Scuseria, M. A. Robb, J. R. Cheeseman, G. Scalmani, V. Barone, B. Mennucci, G. A. Petersson, H. Nakatsuji, M. Caricato, X. Li, H. P. Hratchian, A. F. Izmaylov, J. Bloino, G. Zheng, J. L. Sonnenberg, M. Hada, M. Ehara, K. Toyota, R. Fukuda, J. Hasegawa, M. Ishida, T. Nakajima, Y. Honda, O. Kitao, H. Nakai, T. Vreven, J. A. Montgomery, Jr., J. E. Peralta, F. Ogliaro, M. Bearpark, J. J. Heyd, E. Brothers, K. N. Kudin, V. N. Staroverov, R. Kobayashi, J. Normand, K. Raghavachari, A. Rendell, J. C. Burant, S. S. Iyengar, J. Tomasi, M. Cossi, N. Rega, J. M. Millam, M. Klene, J. E. Knox, J. B. Cross, V. Bakken, C. Adamo, J. Jaramillo, R. Gomperts, R. E. Stratmann, O. Yazyev, A. J. Austin, R. Cammi, C. Pomelli, J. W. Ochterski, R. L. Martin, K. Morokuma, V. G. Zakrzewski, G. A. Voth, P. Salvador, J. J. Dannenberg, S. Dapprich, A. D. Daniels, O. Farkas, J. B. Foresman, J. V. Ortiz, J. Cioslowski and D. J. Fox, Gaussian 09, Revision A.02, *Gaussian Inc.*, Wallingford CT, (2009).
19. S. Kaya, C. Kaya, L. Guo, F. Kandemirli, B. Tüzün, İ. Uğurlu, L. H. Madkour and M. Saracoglu, Quantum chemical and molecular dynamics simulation studies on inhibition performances of some thiazole and thiadiazole derivatives against corrosion of iron, *J. Mol. Liq.*, **219**, 497 (2016).
20. C. G. Zhan, P. S. Spencer, D. A. Dixon, Chromogenic and neurotoxic effects of an aliphatic γ -diketone: Computational insights into the molecular structures and mechanism, *J. Phy. Chem.*, **108**, 6098 (2004).
21. E. E. Ebenso, T. Arslan, F. Kandemirli, I. Love, C. Öğretir, M. Saracoglu and S. A. Umoren, Theoretical studies of some sulphonamides as corrosion inhibitors for mild steel in acidic medium, *Int. J. Quantum Chem.*, **110**, 2614 (2010).
22. M. A. Amin, M. A. Ahmed, H. A. Arida, T. Arslan, M. Saracoglu and F. Kandemirli, Monitoring corrosion and corrosion control of iron in HCl by non-ionic surfactants of the TRITON-X series-Part II. Temperature effect, activation energies and thermodynamics of adsorption, *Corros. Sci.*, **53**, 540 (2011).
23. M. A. Amin, M. A. Ahmed, H. A. Arida, F. Kandemirli, M. Saracoglu, T. Arslan and M. A. Basaran, Monitoring corrosion and corrosion control of iron in HCl by non-ionic surfactants of the TRITON-X series-Part III. Immersion time effects and theoretical studies, *Corros. Sci.*, **53**, 1895 (2011).
24. S. Zor, M. Saracoglu, F. Kandemirli and T. Arslan, Inhibition effects of amides on the corrosion of copper in 1.0 M HCl: Theoretical and experimental studies, *Corrosion*, **67**, 12, 125003 (2011).
25. F. Kandemirli, M. Saracoglu, G. Bulut, E. Ebenso, T. Arslan and A. Kayan, Synthesis and theoretical study of zinc(II) and nickel(II) complexes of 5-methoxyisatin 3-[N-(4-chlorophenyl)thiosemicarbazone], *ITB J. Science (J. Math. and Fund. Sci.)*, **44A**, 35 (2012).
26. M. A. Amin, O. A. Hazzazi, F. Kandemirli and M. Saracoglu, Inhibition performance and adsorptive behaviour of three amino acids on cold rolled steel in 1.0 M HCl-chemical, electrochemical and morphological studies, *Corrosion*, **68**, 688 (2012).
27. F. Kandemirli, M. Saracoglu, M. A. Amin, M. A. Basaran and C. D. Vurdu, The Quantum chemical calculations of serine, threonine and glutamine, *Int. J. Electrochem. Sci.*, **9**, 3819 (2014).
28. M. A. Amin, N. El-Bagoury, M. Saracoglu and M. Ramadan, Electrochemical and corrosion behavior of cast re-containing inconel 718 alloys in sulphuric acid solutions and the effect of Cl⁻, *Int. J. Electrochem. Sci.*, **9**, 5352 (2014).
29. F. Kandemirli, C. D. Vurdu, M. Saracoglu, Y. Akkaya and M. S. Cavus, Some molecular properties and reaction mechanism of synthesized isatin thiosemicarbazone and its zinc(II) and nickel(II) complexes, *Int. Res. J. Pure and Applied Chem.*, **9**, 1 (2015).

30. N. El-Bagoury, M. A. Amin and M. Saracoglu, Effect of aging treatment on the electrochemical and corrosion behavior of nitire shape memory alloy, *Int. J. Electrochem. Sci.*, **10**, 5291 (2015).
31. İ. Ö. İlhan, M. Çadır, M. Saracoglu, F. Kandemirli, Z. Kökbudak and S. Akkoç, The reactions and quantum chemical calculations of some pyrazole-3-carboxylic acid chlorides with various hydrazides, *Chem. Sci. Rev. Lett.*, **4**, 838 (2015).
32. M. A. Amin, S. A. Fadlallah, G. S. Alosaimi, F. Kandemirli, M. Saracoglu, S. Szunerits and R. Boukherroub, Cathodic activation of titanium-supported gold nanoparticles: an efficient and stable electrocatalyst for the hydrogen evolution reaction, *Int. J. Hyd. Energy*, **41**, 6326 (2016).
33. A. Tazouti, M. Galai, R. Touir, M. Ebn Touhami, A. Zarrouk, Y. Ramli, M. Saraçoğlu, S. Kaya, F. Kandemirli and C. Kaya, Experimental and theoretical studies for mild steel corrosion inhibition in 1 M HCl by three new quinoxalinone derivatives, *J. Mol. Liquids*, **221**, 815 (2016).
34. M. A. Amin, M. Saracoglu, N. El-Bagoury, T. Sharshar, M. M. Ibrahim, J. Wysocka, S. Krakowiak and J. Ryl, Microstructure and corrosion behaviour of carbon steel and ferritic and austenitic stainless steels in NaCl solutions and the effect of p-nitrophenyl phosphate disodium salt, *Int. J. Electrochem. Sci.*, **11**, 10029 (2016).
35. M. Saracoglu, F. Kandemirli, A. Ozalp and Z. Kokbudak, Synthesis and quantum chemical calculations of 2,4-dioxopentanoic acid derivatives-part II, *Int. J. Sci. Eng. Inv.*, **6**, 50 (2017).
36. B. Saima, A. Khan, R. Un Nisa, T. Mahmood and K. Ayub, Theoretical insights into thermal cyclophanediene to dihydropyrene electrocyclic reactions; a comparative study of Woodward Hoffmann allowed and forbidden reactions, *J. Mol. Model.*, **22**, 81 (2016).
37. M. Saracoglu, M. I. A. Elusta, S. Kaya, C. Kaya and F. Kandemirli, Quantum chemical studies on the corrosion inhibition of Fe₇₈B₁₃Si₉ glassy alloy in Na₂SO₄ solution of some thiosemicarbazone derivatives, *Int. J. Electrochem. Sci.*, **13**, 8241 (2018).
38. M. Saracoglu, Z. Kokbudak, Z. Çimen and F. Kandemirli, Synthesis and DFT quantum chemical calculations of novel pyrazolo[1,5-c]pyrimidin-7(1H)-one derivatives, *J. Chem. Soc. Pak.*, **41**, 479 (2019).
39. M. Saracoglu, S. G. Kandemirli, A. Başaran, H. Sayiner and F. Kandemirli, Investigation of structure-activity relationship between chemical structure and CCR5 anti HIV-1 activity in a class of 1-[N-(methyl)-N-(phenylsulfonyl)amino]-2-(phenyl)-4-[4-(substituted)piperidin-1-yl] butanes derivatives: The electronic-topological approach, *Curr. HIV Res.*, **9**, 300 (2011).
40. M. Saracoglu, F. Kandemirli, M. A. Amin, C. D. Vurdu, M. S. Cavus and G. Sayiner, The quantum chemical calculations of some thiazole derivatives, Proceedings of the 3rd International Conference on Computation for Science and Technology (ICCST-3), *Published by Atlantis Press*, **5**, 149 (2015).
41. M. Saracoglu, Z. Kokbudak, E. Yalcin and F. Kandemirli, Synthesis and DFT quantum chemical calculations of 2-oxopyrimidin-1(2H)-yl-thiourea and urea derivatives, *J. Chem. Soc. Pak.*, **41**, 841 (2019).
42. K. F. Khaled, Studies of iron corrosion inhibition using chemical, electrochemical and computer simulation techniques, *Electrochim. Acta*, **55**, 6523 (2010).
43. M. J. Dewar and W. Thiel, Ground states of molecules. 38. The MNDO method. Approximations and parameters, *J. Am. Chem. Soc.*, **99**, 4899 (1977).
44. R. G. Pearson, Hard and soft acids and bases-the evolution of a chemical concept, *Coord. Chem. Rev.*, **100**, 403 (1990).
45. L. Pauling, The Nature of the Chemical Bond, *Cornell University Press*, Ithaca, New York, (1960).
46. R. G. Parr and R. G. Pearson, Absolute hardness: Companion parameter to absolute electronegativity, *J. Am. Chem. Soc.*, **105**, 7512 (1983).
47. P. K. Chattaraj, U. Sarkar and D. R. Roy, Electrophilicity index, *Chem. Rev.*, **106**, 2065 (2006).
48. E. E. Ebenso, M. M. Kabanda, T. Arslan, M. Saracoglu, F. Kandemirli, L. C. Murulana, A. K. Singh, S. K. Shukla, B. Hammouti, K. F. Khaled, M. A. Quraishi, I. B. Obot and N. O. Edd, Quantum chemical investigations on quinoline derivatives as effective corrosion inhibitors for mild steel in acidic medium, *Int. J. Electrochem. Sci.*, **7**, 5643 (2012).
49. A. Y. Musa, A. H. Kadhum, A. B. Mohamad, A. B. Rohoma and H. Mesmari, Electrochemical and quantum chemical calculations on 4,4-dimethyloxazolidine-2-thione as inhibitor for mild steel corrosion in hydrochloric acid, *J. Mol. Struct.*, **969**, 233 (2010).
50. K. F. Khaleda and M. M. Al-Qahtani, The inhibitive effect of some tetrazole derivatives towards Al corrosion in acid solution: Chemical,

- electrochemical and theoretical studies, *Mater. Chem. Phys.*, **113**, 150 (2009).
51. Y. C. Guan Luo and K. N. Han, Corrosion inhibition of a mild steel by aniline and alkylamines in acidic solutions, *Corrosion*, **54**, 721 (1998).
52. S. Martinez and I. Štagljar, Correlation between the molecular structure and the corrosion inhibition efficiency of chestnut tannin in acidic solutions, *J. Mol. Struct.*, **640**, 167 (2003).
53. I. B. Obot and N. O. Obi-Egbedi, Adsorption properties and inhibition of mild steel corrosion in sulphuric acid solution by ketoconazole: Experimental and theoretical investigation, *Corros. Sci.*, **52**, 198 (2010).
54. M. M. Solomon, S. A. Umoren, I. I. Udosoro and A. P. Udoh, Inhibitive and adsorption behaviour of carboxymethyl cellulose on mild steel corrosion in sulphuric acid solution, *Corros. Sci.*, **52**, 1317 (2010).
55. A. Rauk, *Orbital interaction theory of organic chemistry*, 2nd ed; Wiley & Sons: New York, (2001).
56. N. O. Obi-Egbedi, I. B. Obot and M. I. El-Khaiary, Quantum chemical investigation and statistical analysis of the relationship between corrosion inhibition efficiency and molecular structure of xanthene and its derivatives on mild steel in sulphuric acid, *J. Mol. Struct.*, **1002**, 86 (2011).
57. M. Djenane, S. Chafaa, N. Chafai, R. Kerkour and A. Hellal, Synthesis, spectral properties and corrosion inhibition efficiency of new ethyl hydrogen [(methoxyphenyl) (methylamino) methyl] phosphonate derivatives: Experimental and theoretical investigation, *J. Mol. Struct.*, **1175**, 398 (2019).
58. J. Bhawsar, P. Jain, M. G. Valladares-Cisneros, C. Cuevas-Arteaga and M. R. Bhawsar, Quantum chemical assessment of two natural compounds: Vasicine and Vasicinone as green corrosion inhibitors, *Int. J. Electrochem. Sci.*, **13**, 3200 (2018).
59. I. B. Obot, N. O. Obi-Egbedi and A. O. Eseola, Anticorrosion potential of 2-Mesityl-1H-imidazo[4,5-f][1,10]phenanthroline on mild steel in sulfuric acid solution: experimental and theoretical study, *Ind. Eng. Chem. Res.*, **50**, 2098 (2011).
60. I. B. Obot, N. O. Obi-Egbedi, E. E. Ebenso, A. S. Afolabi and E. E. Oguzie, Experimental, quantum chemical calculations, and molecular dynamic simulations insight into the corrosion inhibition properties of 2-(6-methylpyridin-2-yl)oxazolo[5,4-f][1,10]phenanthroline on mild steel, *Res. Chem. Intermed.*, **39**, 1927 (2013).
61. R. G. Parr and P. K. Chattaraj, Principle of maximum hardness, *J. Am. Chem. Soc.*, **113**, 1854 (1991).
62. R. G. Pearson, The principle of maximum hardness, *Acc. Chem. Res.*, **26**, 250 (1993).
63. R. G. Pearson, Absolute electronegativity and hardness correlated with molecular orbital theory, *Proceedings of the National Academy of Sciences of the United States of America*, **83**, 8440 (1986).
64. A. Özalp, Z. Kökbudak, M. Saracoglu, F. Kandemirli, İ. Ö. İlhan and C. D. Vurdu, The reactions and quantum chemical calculations of some pyrazole-3-carboxylic acid chlorides with various hydrazides, *Chem. Sci. Rev. Lett.*, **4**, 719 (2015).
65. C. Verma, M. A. Quraishi, K. Kluza, M., Makowska-Janusik, L. O. Olasunkanmi and E. Ebenso, Corrosion inhibition of mild steel in 1 M HCl by D-glucose derivatives of dihydropyrido [2,3-d:6,5-d'] dipyrimidine-2, 4, 6, 8(¹H, ³H, ⁵H, ⁷H)-tetraone, *Sci. Rep.*, **7**, 44432-1 (2017).
66. R. G. Parr, L. V. Szentpaly and S. Liu, Electrophilicity index, *J. Am. Chem. Soc.*, **121**, 1922 (1999).
67. G. Gao and C. Liang, Electrochemical and DFT studies of β-amino-alcohols as corrosion inhibitors for brass, *Electrochim. Acta*, **52**, 4554 (2007).
68. M. Sahin, G. Gece, F. Karci and S. Bilgic, Experimental and theoretical study of the effect of some heterocyclic compounds on the corrosion of low carbon steel in 3.5% NaCl medium, *J. Appl. Electrochem.*, **38**, 809 (2008).
69. M. A. Quraishi and R. Sardar, Hector bases-a new class of heterocyclic corrosion inhibitors for mild steel in acid solutions, *J. Appl. Electrochem.*, **33**, 1163 (2003).
70. N. Khatire-Hamdi, M. Makhloufi-Chebli, H. Grib, M. Brahimi and A. M. S. Silva, Synthesis DFT/TD-DFT theoretical studies and experimental solvatochromic shift methods on determination of ground and excited state dipole moments of 3-(2-hydroxybenzoyl) coumarins, *J. Mol. Struct.*, **1175**, 811 (2019).
71. G. Gece, The use of quantum chemical methods in corrosion inhibitor studies, *Corros. Sci.*, **50**, 2981 (2008).
72. J. N. Murrell, S. F. Kettle and J. M. Tedder, *The Chemical Bond*, John Wiley & Sons, Chichester, UK, (1985).